Electronic Supplementary Information

Multidimensional and hierarchical carbon-confined cobalt phosphide nanocomposite as advanced anodes for lithium and sodium storage

Beibei Wang [ac,1], Kai Chen [a,1], Gang Wang[ac], Xiaojie Liu[bc], Hui Wang[bc*], Jintao Bai [ac*]

[a] *State Key Lab Incubation Base of Photoelectric Technology and Functional Materials, International Collaborative Center on Photoelectric Technology and Nano Functional Materials, Institute of Photonics & Photon-Technology, Northwest University, Xi'an 710069, PR China*

[b] *Key Laboratory of Synthetic and Natural Functional Molecule Chemistry (Ministry of Education), College of Chemistry & Materials science, Northwest University, Xi'an 710127, PR China*

[c] *Shaanxi Joint Lab of Graphene (NWU), Xi'an 710127, PR China*

[*]Corresponding author:

Tel.: +86 029 8836 3115

Fax: +86 029 8830 3798

E-mail address: huiwang@nwu.edu.cn (H. Wang), baijt@nwu.edu.cn

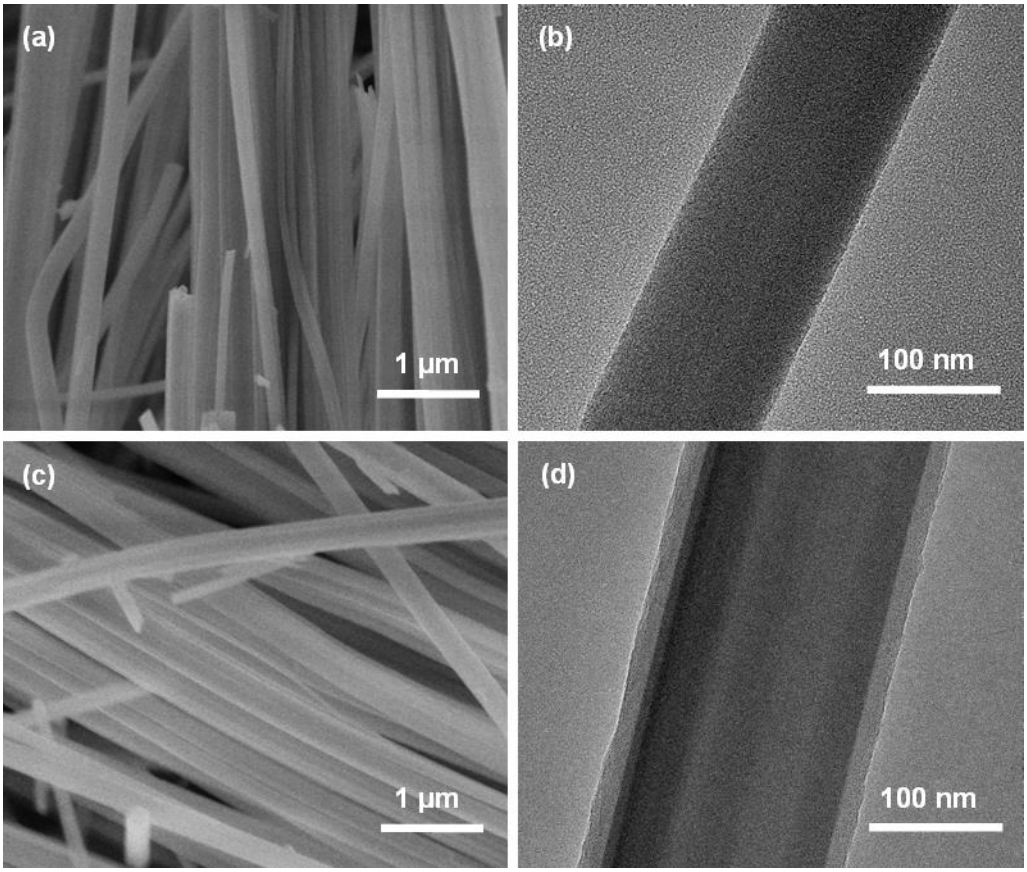

Figure S1 (a and b) SEM and TEM images of (a and b) Co-NAT precursor and (c and d) Co-NTA@hydrotherm carbon nanofibers.

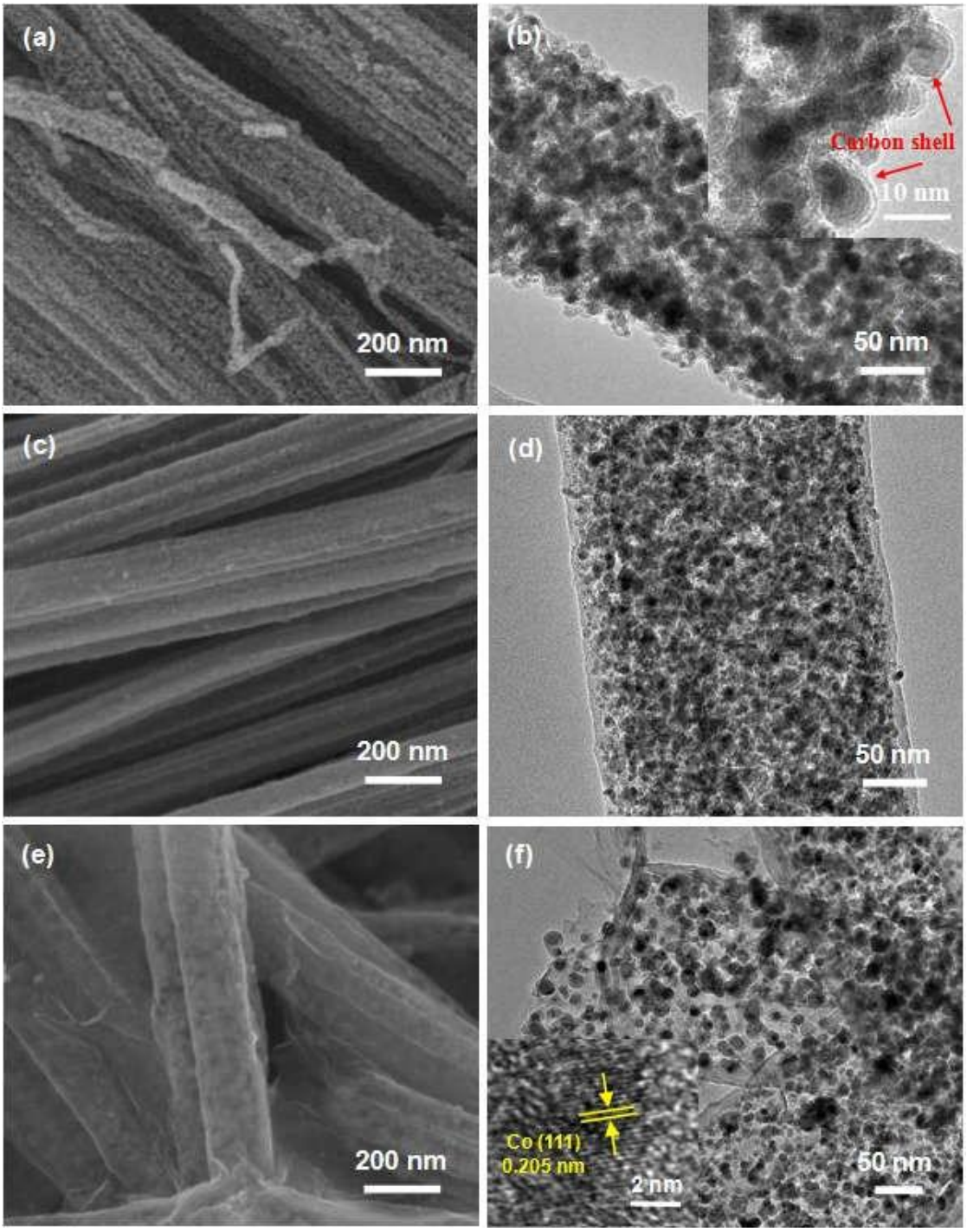

Figure S2 SEM and TEM images of (a and b) Co@C, (c and d) Co@DC and (e and f) Co@DC@GR.

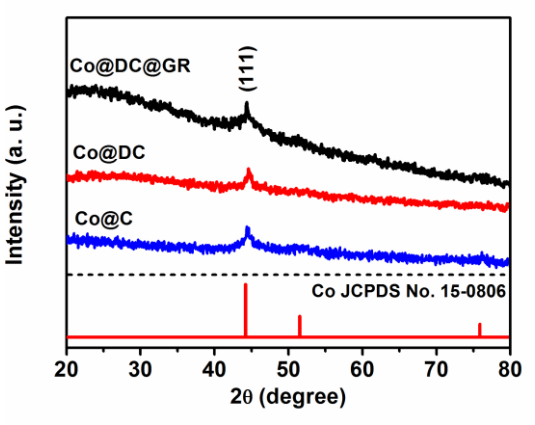

Figure S3 XRD patterns of Co@C, Co@DC and Co@DC@GR.

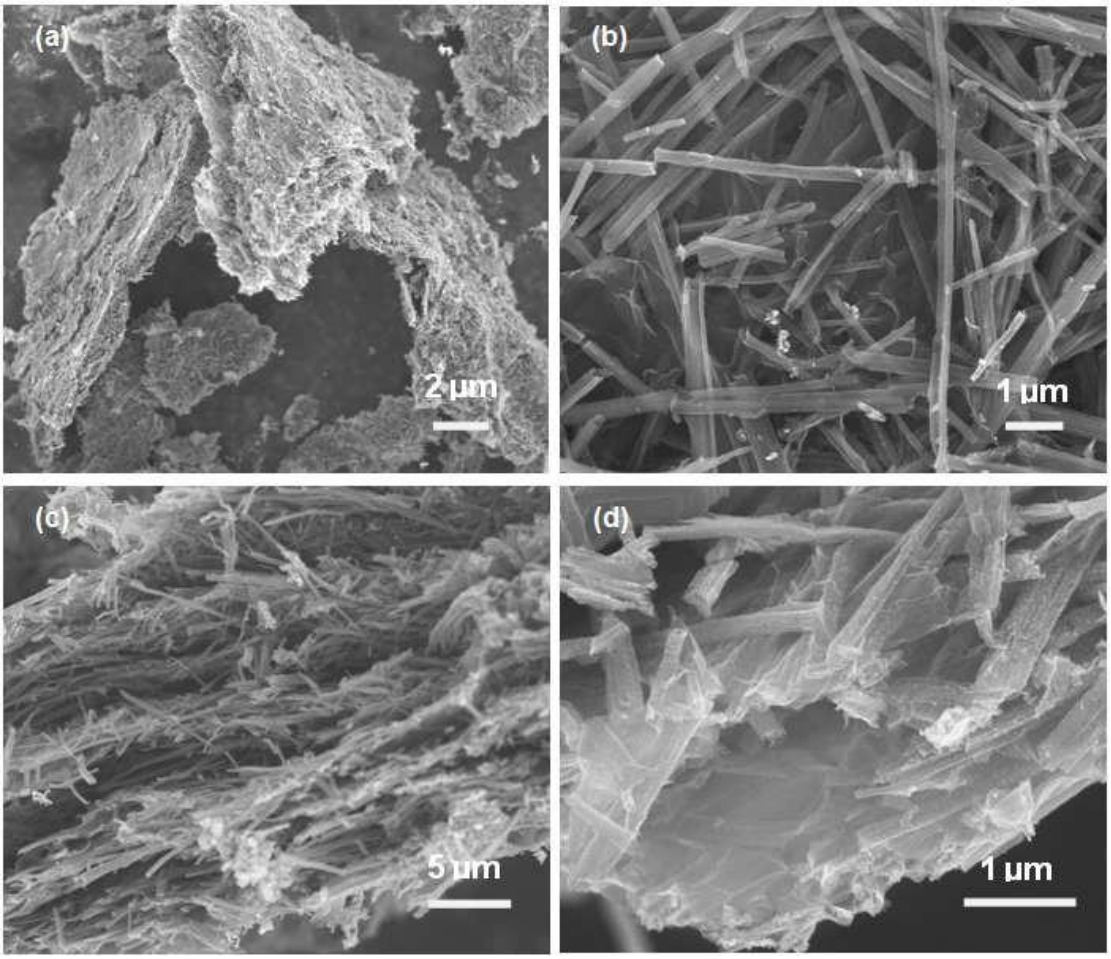

Figure S4 (a and b) low magnification and (c and d) cross-section images of CoP@DC@GR.

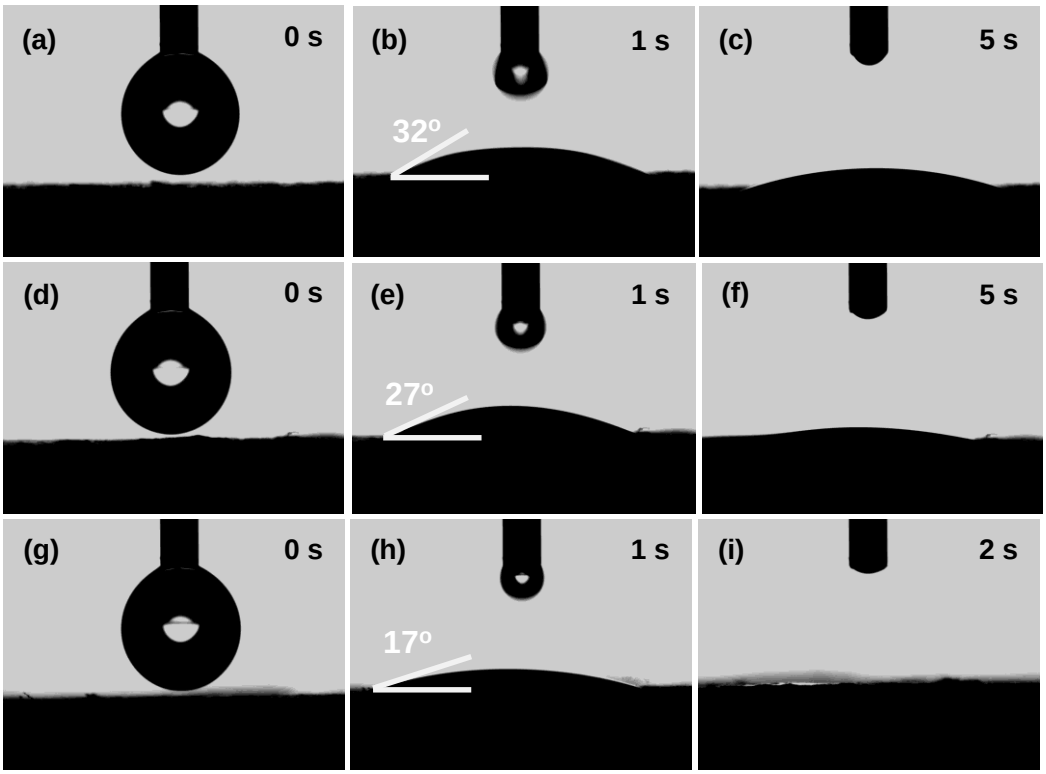

Figure S5. Surface wetting of $LiPF_6$ electrolyte droplet on (a-c) CoP@C, (d-f) CoP@DC and (g-i) CoP@DC @GR.

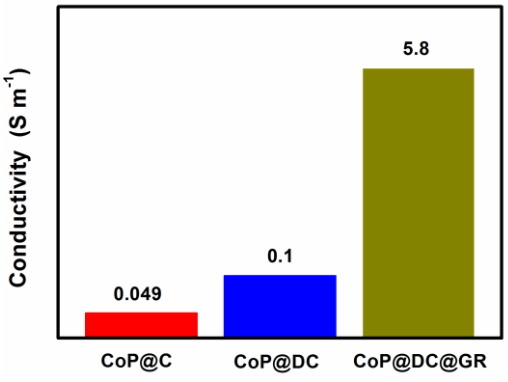

Figure S6 Electrical conductivities of the pressed pellets of CoP@C, CoP@DC and CoP@DC@GR.

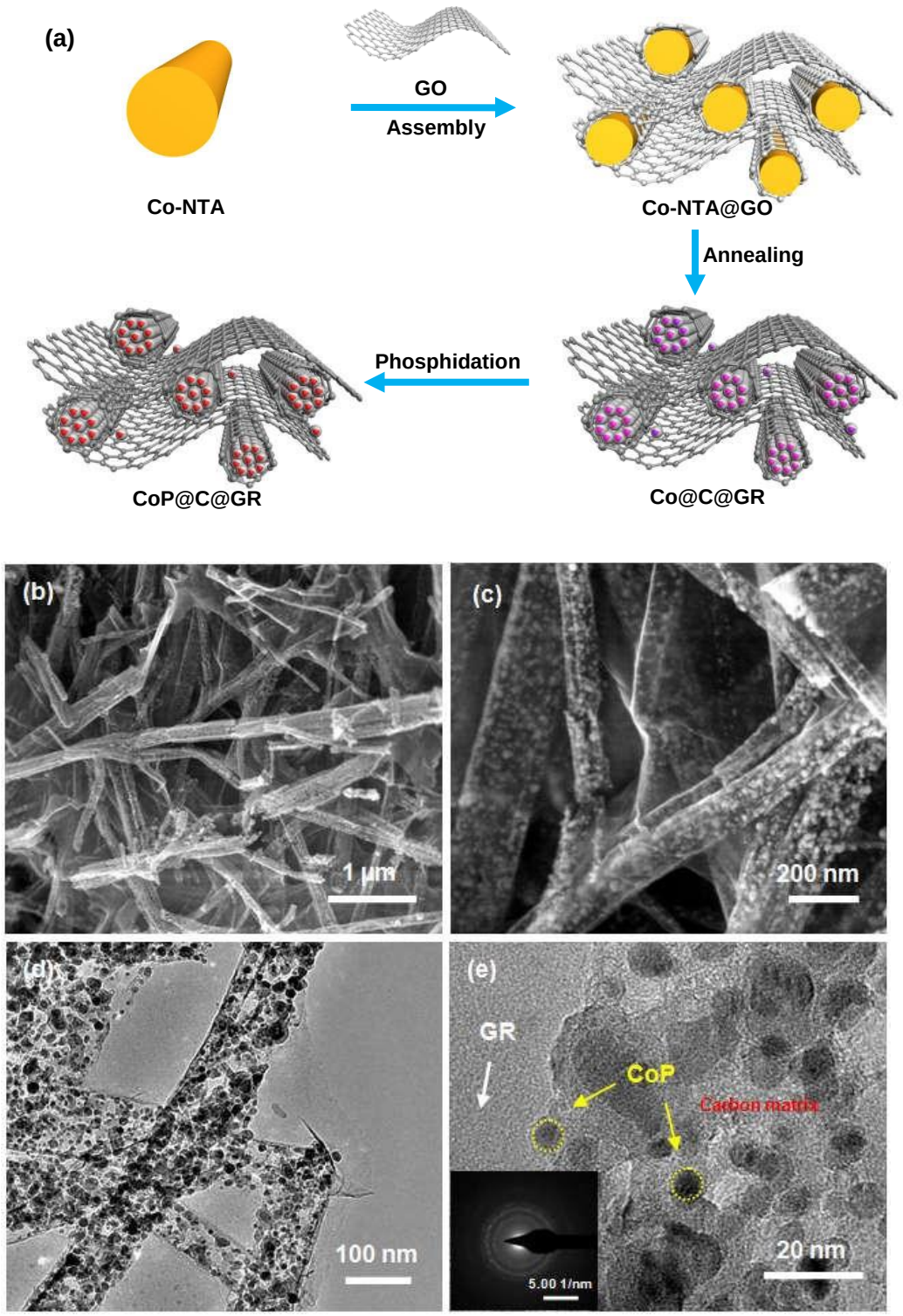

Figure S7 (a) Schematic illustration of the synthesis of CoP@C@GR nanocomposite; (b and c) SEM and (d and e) TEM images of CoP@C@GR nanocomposite.

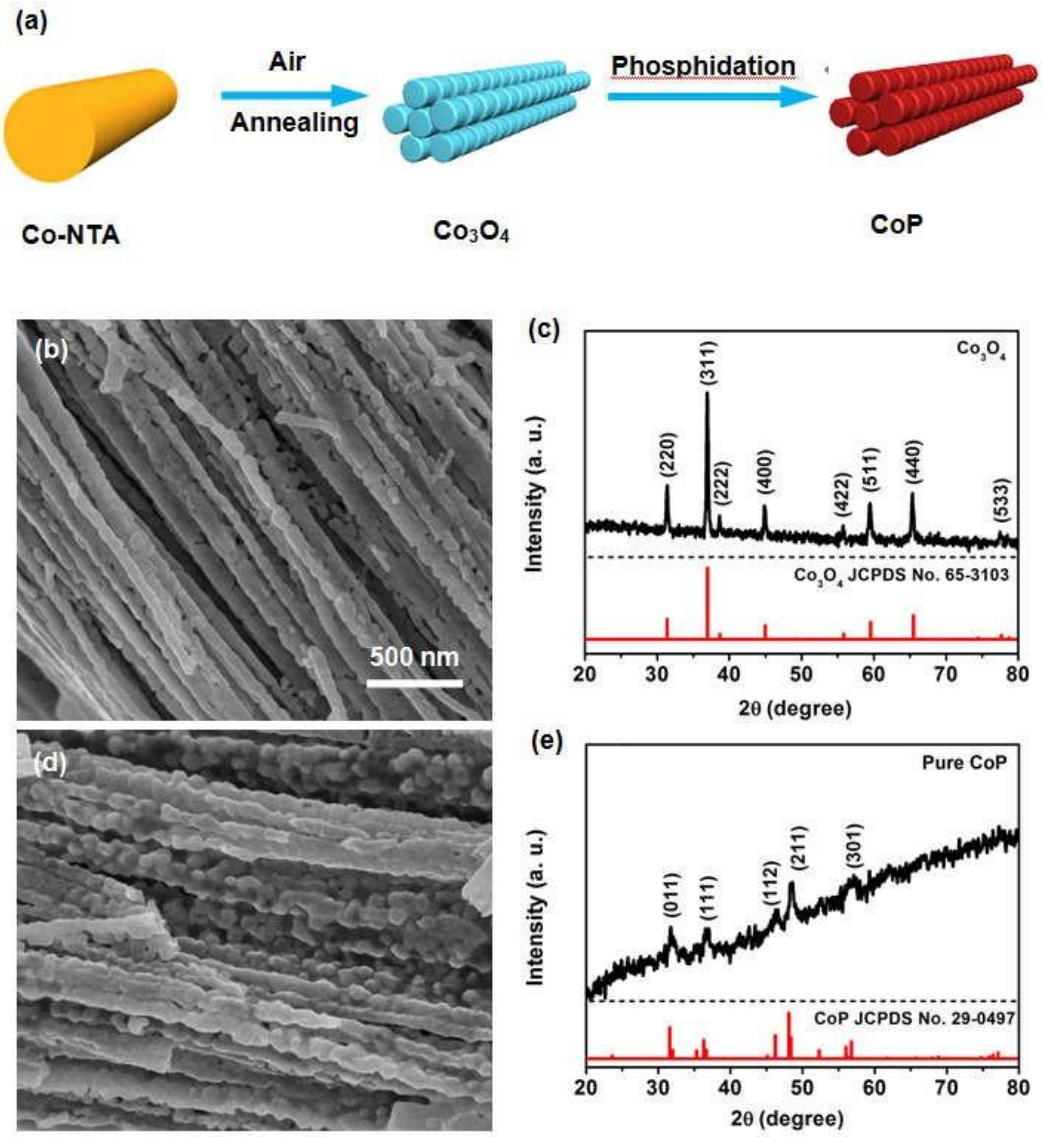

Figure S8 (a) Schematic illustration of the synthesis of pure CoP nanofibers; SEM images of (b) Co_3O_4 nanofibers and (d) pure CoP nanofibers; XRD patterns of (c) Co_3O_4 nanofibers and (e) pure CoP nanofibers.

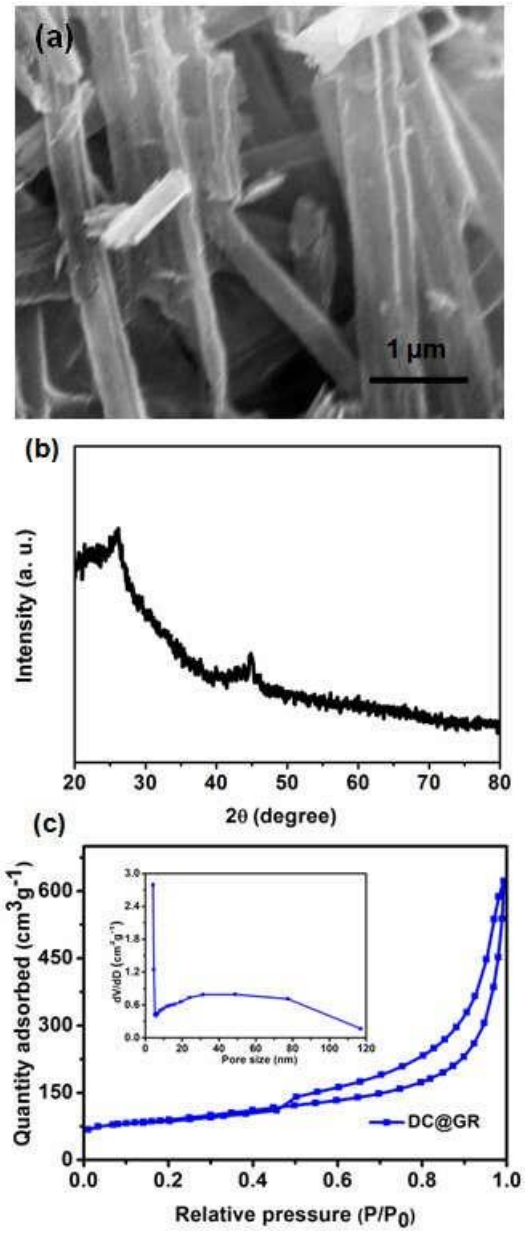

Figure S9 (a) SEM image, (b) XRD pattern and (c) Nitrogen adsorption/desorption isotherms of DC@GR nanocomposite.

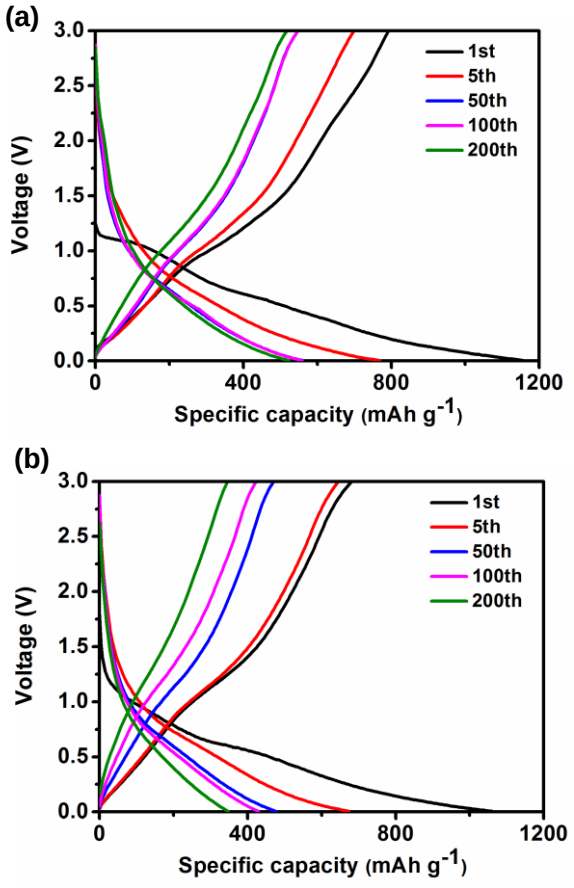

Figure S10 Discharge and charge profiles of (a) CoP@DC and (b) CoP@C electrodes.

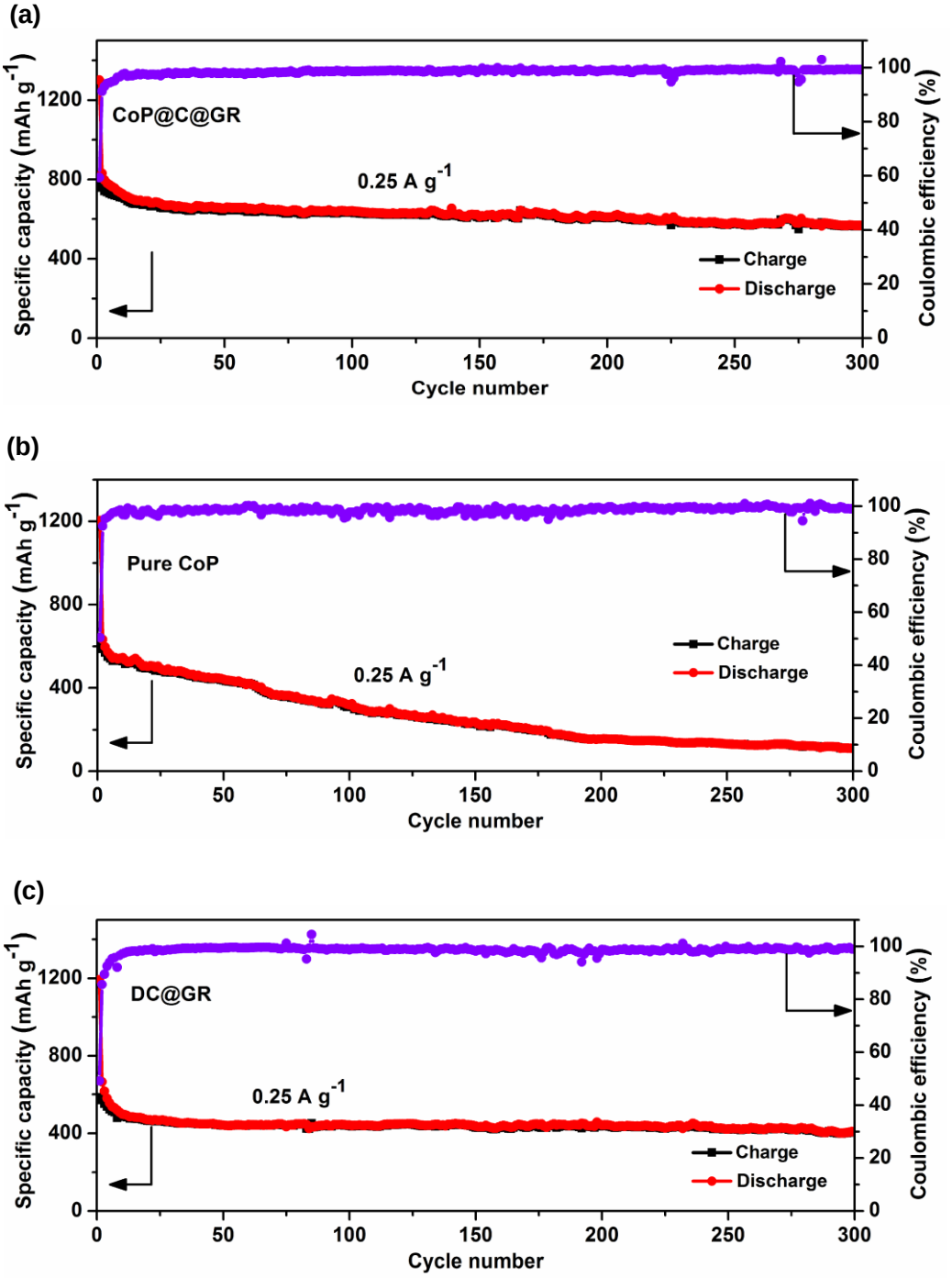

Figure S11 Cycling performance and Coulombic efficiencies of CoP@C@GR, pure CoP and DC@GR at a current density of 0.25 A g^{-1}.

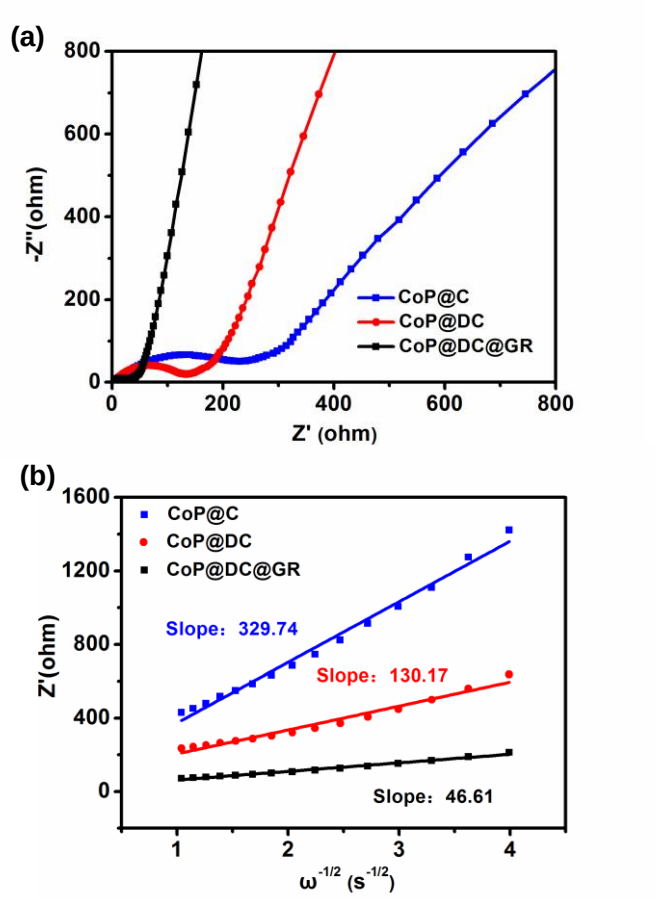

Figure S12 (a) Nyquist plots for the electrodes made of CoP@C, CoP@DC and CoP@DC@GR after 70 cycles at a current density of 0.25 A g^{-1}; (b) Liner fits (relationship between Z' and $\omega^{-1/2}$) in low-frequency region of CoP@C, CoP@DC and CoP@DC@GR electrodes.

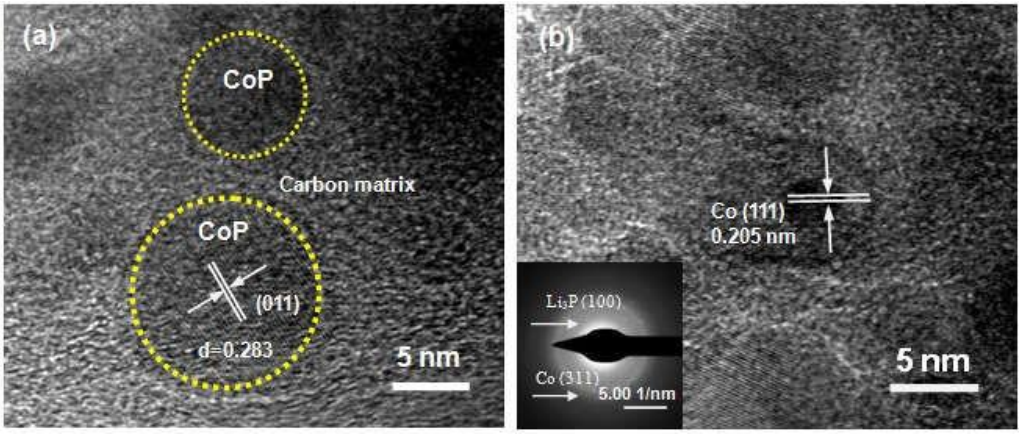

Figure S13 (a) HRTEM image of the fully charged electrode in LIBs; (b) TEM image of the fully discharged electrode in LIBs.

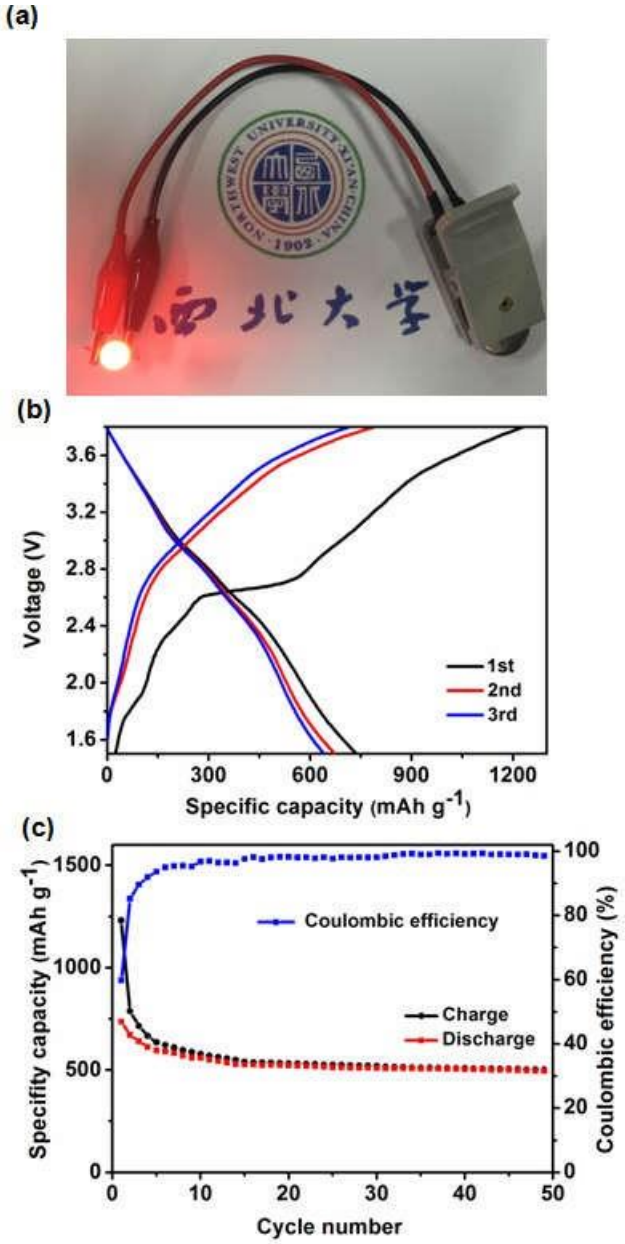

Figure S14 (a) Schematic representation of the CoP@DC@GR//$LiCoO_2$ full-cell; (b) Charge and discharge profiles of the CoP@DC@GR//$LiCoO_2$ full-cell; (c) Cycle performance the CoP@DC@GR//$LiCoO_2$ full-cell.

Table S1 A comparison study of the CoP@DC@GR hybrid nanofibers with other typical phosphide anode materials for SIBs.

Materials	Current density	Specific capacity, cycle number	Ref.
CoP@DC@GR	**0.1 A g^{-1}**	**650 mAh g^{-1},100 cycles**	**This work**
	0.5 A g^{-1}	**398 mAh g^{-1},300 cycles**	
CoP@C-RGO	**0.1 A g^{-1}**	**473 mAh g^{-1}, 100 cycles**	**49**
CoP	**0.1 A g^{-1}**	**315 mAh g^{-1}, 25 cycles**	**50**
Ni_2P⊂pGN	**0.2 A g^{-1}**	**161 mAh g^{-1}, 100 cycles**	**29**
H-FeP@C@GR	**0.1 A g^{-1}**	**400 mAh g^{-1}, 250 cycles**	**16**
Sn_4P_3@C	**0.1 A g^{-1}**	**580 mAh g^{-1}, 120 cycles**	**51**
CuP_2/C	**0.15 A g^{-1}**	**430 mAh g^{-1}, 30 cycles**	**52**
Ni_2P@C/GA	**0.15 A g^{-1}**	**254 mAh g^{-1}, 100 cycles**	**13**

Table S2 The comparison study of lithium and sodium storage for the CoP@DC@GR nanocomposite.

	Lithium storage (0.25 A g^{-1})	Sodium storage (0.1 A g^{-1})
Initial reversible capacity	855 mAh g^{-1}	801 mAh g^{-1}
Initial Coulombic efficiency	73%	64%
Reversible capacity	754 mAh g^{-1} after 300 cycles	650 mAh g^{-1} after 100 cycles
Capacity retention	88%	81%

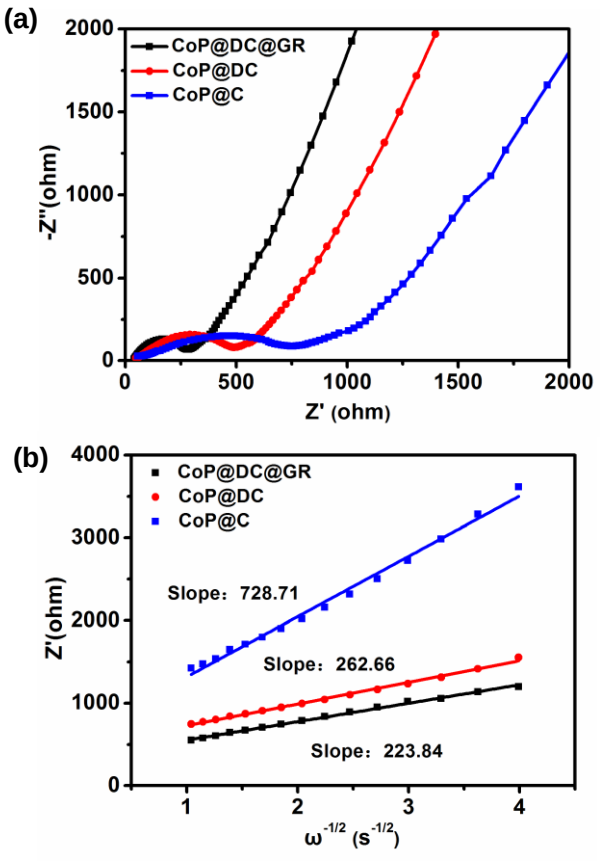

Figure S15 (a) Nyquist plots for the electrodes made of CoP@C, CoP@DC and CoP@DC@GR after 3 cycles for SIBs; (b) Liner fits (relationship between Z' and $\omega^{-1/2}$) in low-frequency region of CoP@C, CoP@DC and CoP@DC@GR electrodes.

Table S3 The comparison study of Rct for CoP@C, CoP@DC and CoP@DC@GR electrodes.

	Electrode	For LIBs	For SIBs
Rct	CoP@C	217 Ω	740 Ω
	CoP@DC	127 Ω	498 Ω
	CoP@DC@GR	45 Ω	257 Ω

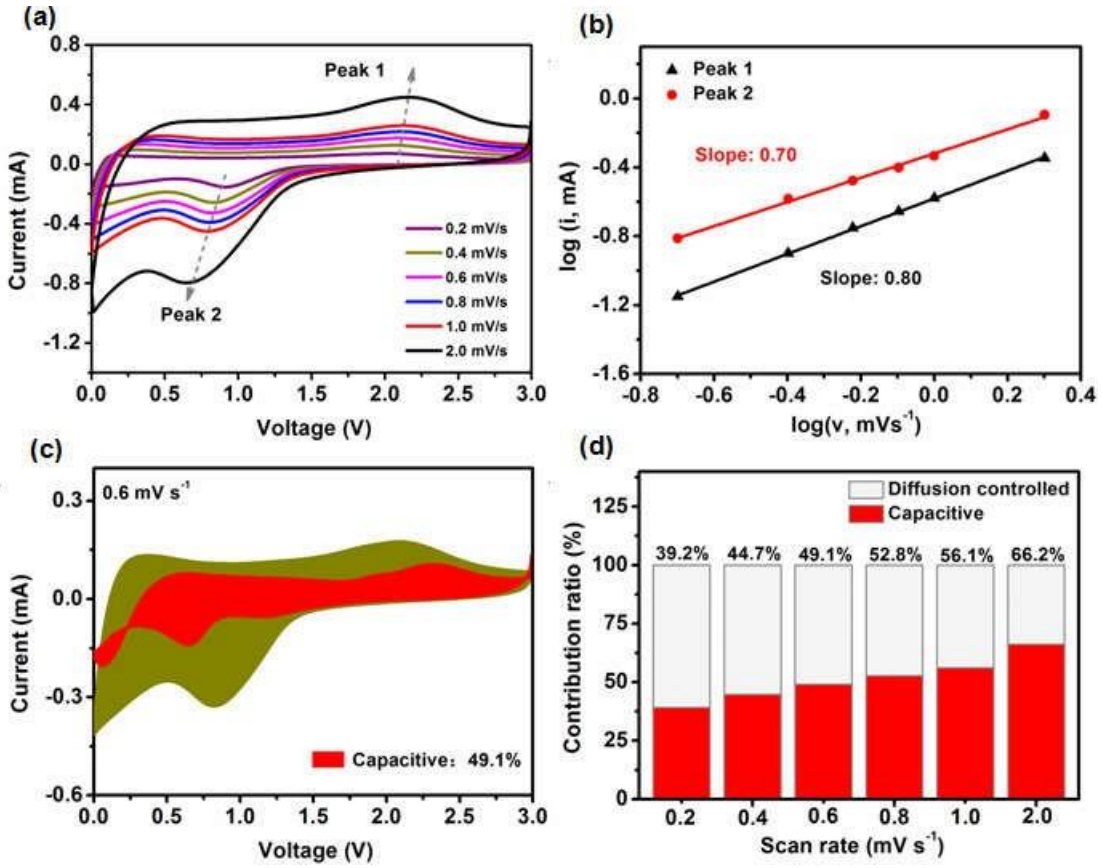

Figure S16. (a) CV curves at different scan rates from 0.2 to 2.0 mV s^{-1} for SIBs; (b) Log i vs. log v plots at oxidation and reduction state; (c) Capacitive- and diffusion-controlled contribution to charge storage at 0.6 mV s^{-1}; (d) Normalized contribution ratio of capacitive- and diffusion-controlled capacities at different scan rates.

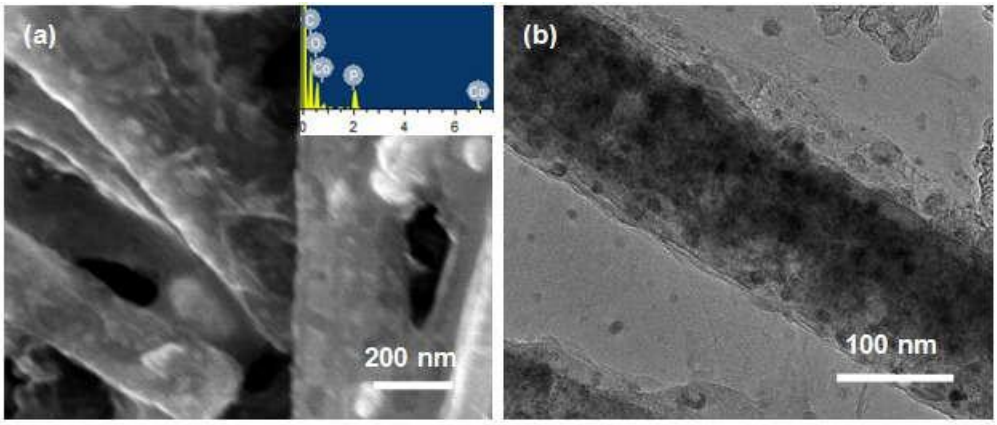

Figure S17 SEM and TEM images of CoP@DC@GR electrode after 100 cycles for SIBs.

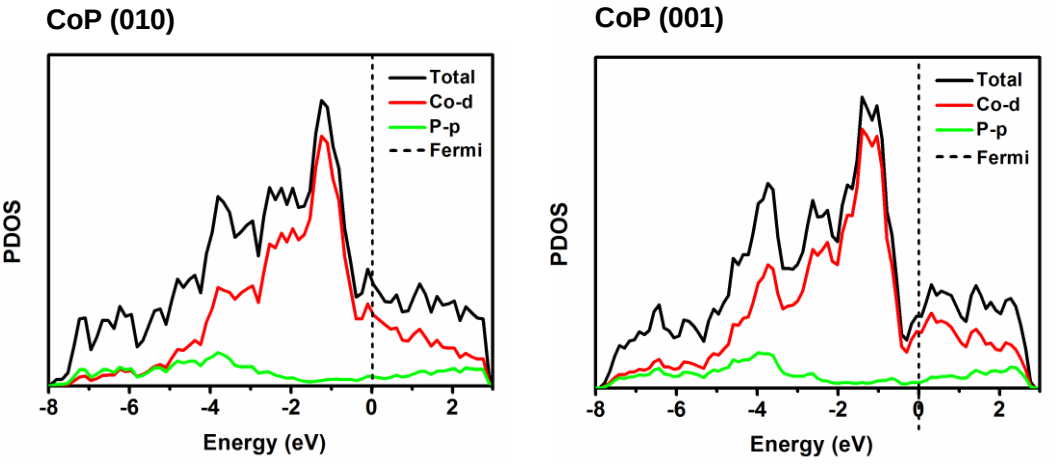

Figure S18 Projected density of states (PDOS) of the CoP surfaces. The Fermi level (dashed line) is set as zero.